Available online at www.sciencedirect.com

ScienceDirect

Procedia Engineering 10 (2011) 894–899

Engineering Procedia

ICM11

Nanofiller Aggregation as Reinforcing Mechanism in Nanocomposites

Andrea Dorigato[a], Yuris Dzenis[b], Alessandro Pegoretti[a*]

[a]*University of Trento, Department of Materials Engineering and Industrial Technologies, via Mesiano 77, 38123, Trento (Italy)*
[b]*Department of Engineering Mechanics, University of Nebraska-Lincoln, W315 Nebraska Hall, USA*

Abstract

A new approach is proposed to model the elastic properties of polymer nanocomposites taking into account agglomeration effects. In particular, the stiffening effect provided by rigid nanoparticles forming primary aggregates is modelled on the hypothesis that part of the polymer matrix is mechanically constrained within the aggregates. To validate the model, linear-low-density polyethylene (LLDPE)/silica micro- and nano-composites have been prepared by melt compounding followed by hot pressing. Electron microscopy observations indicated that the microstructure of the resulting nanocomposites clearly manifested primary aggregation of nanoparticles. Concurrently, thermal calorimetry and X-ray diffraction analyses proved that the crystallization behaviour was not affected by the presence of the filler. Dog-bone specimens have been mechanically tested under uniaxial tension and the data used to validate the model. A good agreement between theoretical predictions and experimental data was demonstrated. The results coupled with the propensity of nanoparticles to form aggregates could explain significant modulus increases in many nanocomposites systems reported earlier.

Keywords: Polyethylene; Nanocomposites; Nanoparticles; Aggregation; Modelling

1. Introduction

A nanocomposite is as a multiphase material where one of the phases has one, two or three dimensions of less than 100 nanometers [1]. As widely reported [2], the dispersion of small quantities (generally less than 5-10 wt%) of nanofillers into polymer matrices can improve their mechanical behavior, gas and

* Corresponding author. Tel.: +39-0461-282452; fax: +39-0461-281977
E-mail address : alessandro.pegoretti@unitn.it

1877–7058 © 2011 Published by Elsevier Ltd.
doi:10.1016/j.proeng.2011.04.147

solvents barrier properties, thermal degradation and chemical resistance, avoiding the typical drawbacks (embrittlement, loss of transparency, loss of lightness) related to traditional microfillers. In particular, it was found that elastic constants of polymer nanocomposites can be dramatically higher than those of the hosting matrix [3]. This reinforcing effect is not predicted by the classical micromechanics models [4] and is most often explained by the formation of an interphase region between the matrix and the particles [5-8]. However, not every polymer-filler system yields extensive interphase. For example, in non polar matrices (such as polyolefins) polymer-filler interactions are usually weak. Relatively little attention was paid to date to another possible reinforcing mechanism in nanocomposites, i.e. nanoparticle aggregation. At the same time, it was demonstrated that aggregation can lead to significant stiffness increases in particulate composites [9]. Nanoparticles have increased general tendency to agglomerate and some nanomanufacturing processes result in strong primary nanoparticles aggregates.

Aim of this work is to investigate the role of the nanofiller aggregation as a possible stiffening mechanism in polymer nanocomposites. The proposed model is validated through experimental measurements performed on polyethylene/silica micro- and nanocomposites.

2. Theoretical background

Hashin and Shtrikman determined [10] the upper and the lower limits of the bulk (K^*) and shear (G^*) modulus of isotropic composite material comprising a matrix (m) and a filler (f) with the corresponding volume fractions (V_m, V_f), for $K_f > K_m$ and $G_f > G_m$ as:

$$K_m + \frac{V_f\left(K_f - K_m\right)}{1 + V_m R_m\left(K_f - K_m\right)} \le K^* \le K_f + \frac{V_m\left(K_m - K_f\right)}{1 + V_f R_f\left(K_m - K_f\right)} \qquad (1)$$

$$G_m + \frac{V_f\left(G_f - G_m\right)}{1 + V_m Q_m\left(G_f - G_m\right)} \le G^* \le G_f + \frac{V_m\left(G_m - G_f\right)}{1 + V_f Q_f\left(G_m - G_f\right)} \qquad (2)$$

with $R_i = 3/(3K_i + 4G_i)$ and $Q_i = [6(K_i + 2G_i)]/[5G_i(3K_i + 4G_i)]$, and i indicating the two phases (m, f). The microstructure of particulate nanocomposites is often characterized by the presence of large (more than 100 nm wide) aggregates of primary nanoparticles homogeneously dispersed in the matrix (Fig 1).

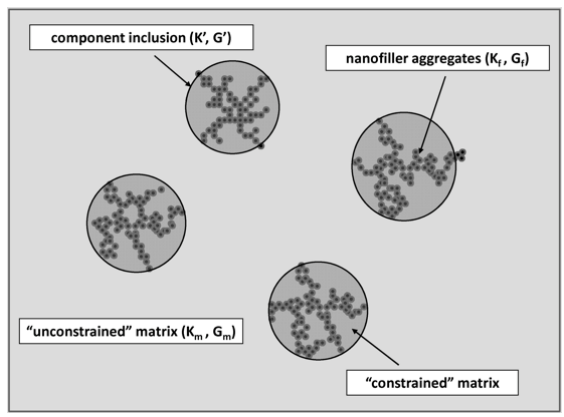

Fig. 1. Schematic representation of the structure of a particulate composite with primary particle aggregation.

It was shown [10] that deformation of the matrix confined within these aggregates is constrained by the rigid neighboring particle chains and the mechanical properties of the compound inclusions can be described by the upper bounds of the moduli (Eqs. 1 and 2). In the case of primary aggregates considered here, the matrix can be then separated into a fraction m_1 of free (unconstrained) polymer matrix and a fraction m_2 of matrix constrained within the aggregates. It is therefore possible to define a new structural parameter $\alpha = m_2 / V$, as the ratio between the volume fraction of constrained matrix (m_2) and the filler amount (V). In order to determine the bulk modulus of the composite (K^*), it is necessary to calculate the bulk modulus of the inclusion (K'), referring to the upper limit reported in Equation (1). Now, K^* can be then determined with the following expression [9]:

$$K^* = K_m + \frac{V'(K' - K_m)}{1 + (1 - V')R_m(K' - K_m)} \qquad (3)$$

where $V' = V + m_2 = V(1+\alpha)$ represents the volume fraction of the inclusion. Substituting the expression of K' in Equation (3) and simplifying, the bulk modulus of the composite will be given by:

$$K^* = K_m + \frac{V'(K_f - K_m)}{1 + (1 - V')R_m(K_f - K_m) + R} \qquad (4)$$

where $R = \alpha / [1 + R_f(K_m - K_f)]$, with $R_f = 3 / [3K_f + 4G_f]$. By a similar approach we can estimate the shear modulus (G^*) [9] and, assuming isotropic material symmetry, the elastic modulus of the composite (E*) as:

$$E^* = \frac{9K^*G^*}{3K^* + G^*} \qquad (5)$$

The parameter α can be evaluated a posteriori by fitting the experimental data.

3. Experimental

A Flexirene® CL10 linear low density polyethylene (density 0.917 g·cm^{-3}, melt flow index at 190 °C and 2.16 kg equal to 2.6 g·(10min)$^{-1}$), kindly supplied by Polimeri Europa SpA (Mantova, Italy), was utilized as polymer matrix. Traditional microcomposites were prepared by using Cores® silica glass microspheres, while two different kinds of fumed silica nanoparticles, Aerosil® 200 and Aerosil® 380 by Evonik (Dusseldorf, Germany), were considered for the preparation of nanocomposites. Fumed silica nanopowders are designated with the letter A followed by the indication of the surface area, while glass microspheres are simply denoted as Glass. Some physical properties of the fillers are listed in Table 1.

Table 1 Physical properties of fumed silica nanoparticles and glass microbeads utilized in this work.

Filler	Density (g·cm^{-3})	BET surface area (m^2·g^{-1})	Primary nanoparticles size
Glass	2.43 ± 0.01	0.5 ± 0.1	18 μm
A200	2.27 ± 0.02	196.6 ± 1.7	12 nm
A380	2.41 ± 0.02	320.8 ± 3.4	7 nm

Density measurements were performed by using a Micromeritics Accupyc® 1330 helium pycnometer (T = 23 °C)
Surface area and porosity were determined by an ASAP® 2010 Accelerated Surface Area and Porosimetry machine.

Both micro- and nanocomposites were melt compounded with the matrix in a Thermo Haake internal mixer, at 170 °C for 15 min and 90 rpm followed by hot pressing in a Carver® laboratory press at 170 °C. Filler volume fraction was varied between 0.01 and 0.04. The composites are designated with the name of the matrix (LLDPE), followed by the name of the filler and its volume content. For example, LLDPE-A200-2 indicates a nanocomposite containing 2 vol% of Aerosil 200 fumed silica.

Cryofractured surfaces of LLDPE-Glass-2 sample were observed by an optical microscope, while ultramicrotomed thin sections of undeformed LLDPE-A380-2 sample were observed by a Philips FEI CM120 transmission electronic microscope (TEM). Differential scanning calorimetry (DSC) were performed by using a Mettler® DSC30 differential scanning calorimeter, in a temperature range from 0 °C to 200 °C at a heating rate of 10 K·min^{-1}, under a nitrogen flow of 100 ml·min^{-1}. In order to evaluate the influence of the fillers on the crystalline structure of the material, X-Ray diffraction analysis was also conducted. A Rigaku® 3D Max X-Ray diffractometer was used, scanning the samples in a 2θ range between 1° and 67°, at a 2θ step of 0.1°. The wavelength of the X-Ray source was 0.154056 nm. From the diffractograms it was possible to determine the dimensional distribution of the crystalline domains, on the basis of an algorithm for whole powder pattern modeling (WPPM) [11]. Uniaxial tensile tests were performed with an Instron 4502 testing machine on ISO 527 type 1BA specimens, at a crosshead speed of 0.25 mm·min^{-1}. The strain was recorded by using a resistance extensometer Instron model 2620-601 (gage length = 12.5 mm).

4. Results and discussion

The optical image of Fig 2a shows that LLDPE-Glass-2 microcomposite is characterized by the presence of microspheres homogeneously dispersed within the matrix, having a mean diameter of about 20 μm. On the other hand, the TEM picture of Fig 2b indicates that in the nanocomposite sample the primary nanoparticles are organized in aggregates with a mean diameter of about 100-200 nm.

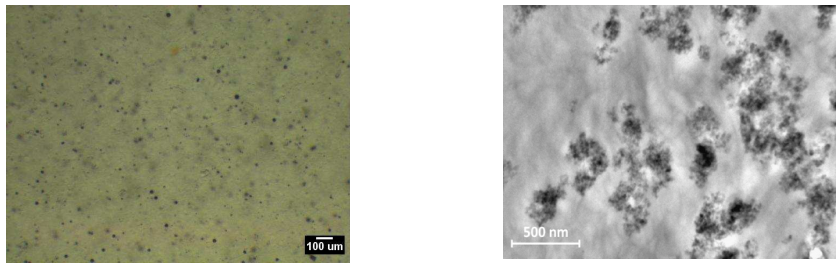

(a) (b)

Fig. 2. (a) ESEM image of LLDPE-Glass-2 microcomposite; (b) TEM image of LLDPE-A380-2 nanocomposite

From XRD and DSC tests we can conclude that the melting temperature, the crystallinity and the mean dimension of the crystallites are not influenced by the presence of the nanofiller. This result can be probably attributed to the amorphous nature of the silica particles utilized in this work.

The relative elastic modulus of the prepared composites is plotted in Fig 3a as a function of the filler volume fraction, along with the fitting curves obtained with the proposed model. In the case of microcomposites the stiffening effect is rather weak, while for nanofilled samples a remarkable enhancement of the elastic modulus was detected, especially by using high surface area nanosilica (A380) at elevated filler amounts. It can be noticed that the proposed model can quite satisfactory predict the tensile elastic modulus of the prepared composites over the whole range of the considered compositions. The modest elastic modulus increase detected for microcomposites is associated to a very low α value (0.3), indicating that only a small (virtually zero) fraction of the matrix is constrained by microparticles. On the contrary, the noticeable increase of the elastic modulus detected for nanocomposites is accompanied by elevated α values (5.1 for A200 and 7.6 for A380). It is interesting to observe that there exists an apparent correlation between the α parameter and filler surface area. The amount of mechanically constrained matrix should depend primarily on the morphology and extent of aggregates and shouldn't necessarily correlate with particle surface area. However, it's well-known that smaller particles (i.e. particles with higher surface area) have stronger propensity to agglomerate and the observed apparent correlation might be the result of more extensive primary aggregates formed during manufacturing of finer fumed silica filler. Indeed, it was reported by Gun'ko et al. that particle aggregation correlated with increasing specific surface area of fumed silicas [12].

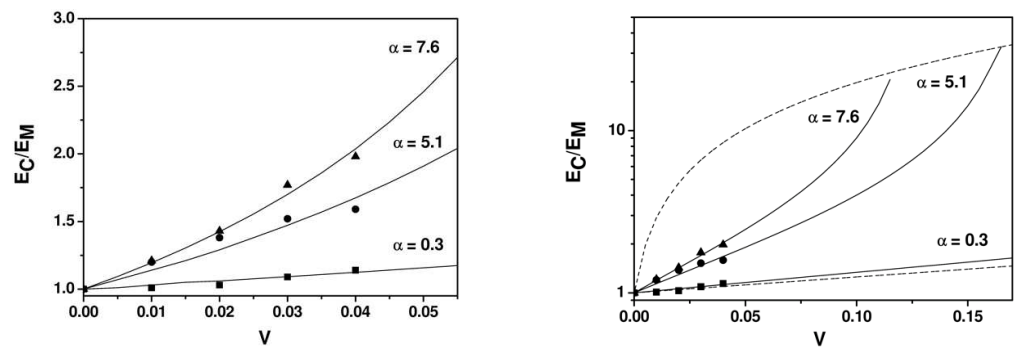

(a) (b)

Fig. 3. Relative elastic modulus of LLDPE silica micro- and nanocomposites as a function of the filler volume content. (■) LLDPE-Glass-x, (●) LLDPE-A200-x, (▲) LLDPE-A380-x. (a) Fitting of experimental data according to the proposed model (continuous line, Eqs. 3-5); (b) comparison with the upper and lower limits according to Eqs. 1, 2 (dashed line).

In Fig 3b elastic modulus data are compared with the limits imposed by Hashin-Shtrikman equation (Eqs. 1 and 2). The theoretical upper limit is reached at different concentrations depending on the fillers surface area. A threshold concentration V_∞, at which all the matrix is in a constrained state can be identified. It is worthwhile to note that V_∞ values for nanocomposites are lower than 20 vol%, thus justifying the noticeable modulus increment detected even at low filler contents.

On the basis of these preliminary results we believe that the proposed approach, taking into account the propensity of nanoparticles to form aggregates, could explain significant observed modulus increases in many nanocomposites systems reported earlier. Primary aggregation considered here may be present without or with interphase formation and, at higher concentrations, can be accompanied with secondary (dynamic) agglomeration leading to percolation [10].

5. Conclusions

A new model is proposed to fit elastic modulus data of LLDPE-amorphous silica micro- and nanocomposites, prepared through a melt compounding process by varying the filler content and the filler dimensions. Considering that DSC and XRD techniques do not evidence any influence of silica fillers on the crystallinity of the matrix, the noticeable enhancements of the elastic modulus detected for nanofilled samples can not be attributed to modification of the matrix microstructure. On the other hand, microscopy techniques revealed an extended primary aggregation of the nanoparticles. Therefore, a new model, taking into account the presence of a portion of constrained matrix within silica aggregates, is successfully introduced to fit elastic modulus data obtained from quasi-static tensile tests. A good agreement between theoretical prediction and experimental data emerged for both the microcomposites and the nanofilled samples.

References

[1] Ajayan PM, Schadler LS, Braun PV. Nanocomposite Science and Technology. Weinheim, Germany: Wiley-VCH Verlag GmbH Co. KGaA; 2003.
[2] Gupta RK, Kennel E, Kim K-J. Polymer Nanocomposites Handbook. Boca Raton, FL: CRC Press; 2010.
[3] Manias E. Nanocomposites. Stiffer by design. *Nat Mater* 2007;**6**:9-11.
[4] Christensen RM. *Mechanics of Composite Materials*. New York: Dover Publications; 2005.
[5] Alberola ND, Benzarti K, Bas C, Bomal Y. Interface effects in elastomers reinforced by modified precipitated silica *Polym Compos* 2001;**22**:312-25.
[6] Colombini D, Hassander H, Karlsson OJ, Maurer FHJ. Influence of the particle size and particle size ratio on the morphology and viscoelastic properties of bimodal hard/soft latex blends. *Macromolecules* 2004;**37**:6865-73.
[7] Lutz MP, Zimmermann RW. Effect of an inhomogeneous interphase zone on the bulk modulus and conductivity of a particulate composite. *International Journal of Solids Structures* 2005;**42**:429-37.
[8] Sevostianov I, Kachanov M. Effect of interphase layers on the overall elastic and conductive properties of matrix composites. Applications to nanosize inclusion. . *International Journal of Solids Structures* 2007;**44**:1304-15.
[9] Dzenis Y. Effect of aggregation of a dispersed rigid fillller on the elastic characteristics of a polymer composite. *Mech Compos Mater* 1986;**22**:14-22.
[10] Hashin Z, Shtrikman S. A variational approach to the theory of the elastic behaviour of multiphase materials *Journal of Mechanics and Physics of Solids* 1963;**11**:127-40.
[11] Scardi P, Leoni M. Whole powder pattern modelling. *Acta Crystallographica* 2002;**A58**:190-200.
[12] Gun'ko VM, Mironyuk IF, Zarko VI, Voronin EF, Turov VV, Pakhlov EM, et al. Morphology and surface properties of fumed silicas. *J Colloid Interface Sci* 2005;**289**:427-45.